ISSN 0006-3509, Biophysics, 2018, Vol. 63, No. 4, pp. 621–628. © Pleiades Publishing, Inc., 2018.
Original Russian Text © V.L. Bopp, N.A. Mistratova, E.A. Petrakovskaya, Yu.L. Gurevich, M.I. Teremova, R.G. Khlebopros, 2018, published in Biofizika, 2018, Vol. 63, No. 4, pp. 786–794.

COMPLEX SYSTEMS BIOPHYSICS

The Influence of Nanoparticles of Biogenic Ferrihydrite on the Rooting of Lignified Cuttings of the Ledebour Willow

V. L. Bopp[a], *, N. A. Mistratova[a], E. A. Petrakovskaya[b], Yu. L. Gurevich[b], **, M. I. Teremova[b], and R. G. Khlebopros[b], †

[a] *Krasnoyarsk State Agrarian University, Krasnoyarsk, 660049 Russia*

[b] *Krasnoyarsk Science Center Federal Research Center, Siberian Branch, Russian Academy of Sciences, Krasnoyarsk, 660036 Russia*

**e-mail: vl_kolesnikova@mail.ru*

***e-mail: btchem@mail.ru*

Received March 13, 2018; in final form, April 19, 2018

Abstract—The influence of nanoparticles of biogenic ferrihydrite on the root formation of lignified cuttings of the Ledebour willow (*Salix ledebouriana* Trautv.) was investigated. The rooting of stem cuttings was performed in water using a phytohormone (indoyl-3-acetic acid) and nanoparticles. In comparison with the variants of incubation of cuttings in water and in a solution containing indolyl-3-acetic acid, the number and total length of the adventitious roots after 5 and 15 days of rooting were greatest in the cuttings treated with nanoparticles. In the early period of root development, increased levels of free radicals and intensities of the hyperfine structure lines of Mn^{2+} cleavage were recorded in the EPR spectra of plant tissues (lenticels of cuttings of treated with nanoparticles). The latter is related to the activity of manganese-containing superoxide dismutase. The response of cuttings to the treatment with nanoparticles was recorded by EPR before manifestation of adventitious root primordium initiation and development.

DOI: 10.1134/S0006350918040036

INTRODUCTION

Nanoparticles of natural and artificial origins and of different natures are often found in the environment. In view of this, the effects of nanoparticles of metals, metal oxides (Fe, Zn, Al, Ti, etc.), nanotubes, fullerenes, etc., on plant growth have been studied for a number of years [1–5]. The most important factors that determine the soil state include the iron-containing compounds [6], which are present in the form of hydroxides and oxides. Soils that are exposed to weathering and contain dissolved metal cations usually accumulate poorly crystallized nanosized iron hydroxide, ferrihydrite. Ferrihydrite can be deposited on the root surface [7]. Its formation is facilitated by soluble organic substances in the rhizosphere of plants, such as citric acid or other compounds that form complexes with iron ions [8, 9]. Due to a large specific surface area (up to 700 $m^2\ g^{-1}$) and sorption capacity, it has a significant effect on the mobility of chemical elements [10]. By absorbing heavy metal ions, herbicides, and other organic compounds [11, 12], iron oxides and hydroxides reduce their toxicity to plants. Studies of the interaction of nanoparticles with living organisms focus primarily on their toxicity [1, 2, 13]. However, the positive effects of the interaction of nanoparticles with plants [14] and other living organisms have also been reported. The ambiguity of the effect of nanoparticles on plant growth was noted in several studies [15–17].

The cytotoxicity and phytotoxicity of nanoparticles is often attributed to elevated levels of reactive oxygen species (ROS) [5, 18, 19]. In oxidative stress, ROS induce lipid peroxidation, membrane destruction, and damage of DNA and proteins. However, ROS are also involved in the regulation of expression of some genes and control plant growth processes such as the cell cycle, rooting, and growth of the aboveground parts [20–23]. These effects of nanoparticles on plant cells probably determine the manifestation of the positive responses of plants. Comprehensive studies are required to elucidate the mechanisms of the biological activities of nanoparticles and the ambiguity of the effects of their interaction with plants. The goal of this study was to analyze the effect of biogenic ferrihydrite nanoparticles on rhizogenesis (rooting) of lignified cuttings of the Ledebour willow and on the level of reactive oxygen species.

Abbreviations: ROS, reactive oxygen species; IAA, indolyl-3-acetic acid; FFE, full factorial experiment; EPR, electron paramagnetic resonance; EMR, electron magnetic resonance; Mn-SOD, manganese-containing superoxide dismutase.

† Deceased.

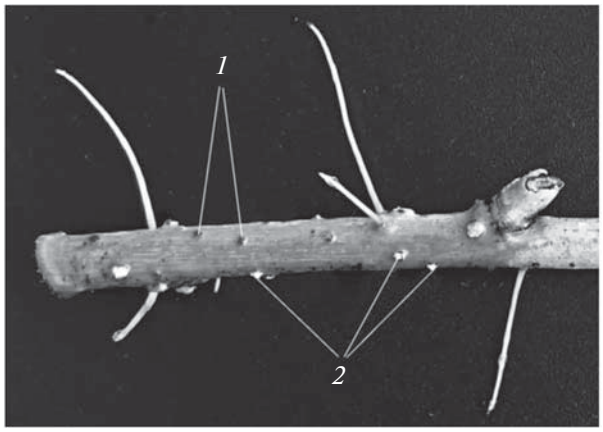

Fig. 1. Photograph of Ledebour willow lignified cuttings at the initial stage of rooting (5 days): (*1*) dormant lenticels; (*2*) hypertrophied lenticels.

MATERIALS AND METHODS

In these experiments, we used lignified cuttings of the Ledebour willow (*Salix ledebouriana* Trautv.), which were obtained by the standard procedure [24]. Cuttings 20 cm long, which were selected for the experiment in March, were immersed for some time in an aqueous solution of indole-3-acetic acid (IAA) and in the same solution containing biogenic ferrihydrite nanoparticles. The cuttings were then transferred into water and after the formation of adventitious roots were planted in open ground. The concentration of nanoparticles (X_1) and the exposure time of the cuttings in the solutions containing the phytohormone and nanoparticles (X_2) were determined using the planning matrix for a full factorial experiment (FFE) 2^2 with a central point [25]. The interval of variation ($\pm\lambda$) was selected as 0.5 mg/L for X_1 and 3 h for X_2. In the central point of the plan of experiments, the values of the factors X_1 and X_2 were selected as 1 mg/L and 13 h, respectively. The rooting efficiency (Y) criterion was the number and total length of adventitious roots of the first branching order. The biometric parameters of the root system (the number and length of roots) were determined according to V.F. Moiseichenko [26]. Determinations were performed on rooting days 5 and 15. The data were statistically processed and the plots were constructed using the Statistica 6.0 software package (StatSoft, United States).

Biogenic ferrihydrite nanoparticles were obtained in the culture of aerobic bacteria isolated from Middle-Timan bauxites [27]. The bacteria were selected in a mineral medium containing iron citrate as the sole carbon and energy source. According to the results of sequencing and analysis of the 16S rRNA gene fragment, the selected strain was identified as *Delftia tsuruhatensis* T7 on the basis of 99.345% similarity. The bacteria were cultured in the batch mode in a 2.5-L reactor with aeration and mechanical stirring at 500 rpm at 32°C. The nutrient medium contained the following mineral salts: 0.4 g/L NH_2SO_4, 0.05 g/L K_2SO_4, 0.05 g/L $MgSO_4 \cdot 7H_2O$, 0.02 g/L $NaH_2PO_4 \cdot 12H_2O$, 0.02, and 6.0 g/L iron citrate, which was dissolved in distilled water (initial pH 6.3). Culturing was performed for 2–4 days.

The material obtained after the end of culturing of the bacteria was pelleted by centrifugation at 4000 rpm, the pellet was transferred to double-distilled water and sonicated at 22 kHz and 8 W/cm^2 (UZTA-0.4/22-OM generator, Russia). The homogenate was centrifuged at 18500 *g* for 30 min, the supernatant (colloidal nanoparticle solution) was decanted and used in experiments. According to powder X-ray diffraction and Mossbauer spectroscopy data, the nanoparticles were formed by ferrihydrite. The diameter of nanoparticles, which was determined by small-angle X-ray scattering, was 2–10 nm [27]. In soils, they are present as both individual nanoparticles and nanoscale aggregates with a hydrodynamic diameter of 2 to 200 nm [28].

Electron paramagnetic resonance (EPR) spectra of plant-tissue samples were recorded with an ELEXYS E580 X-band spectrometer (Bruker Biospin GmbH, Germany). To record the spectra, the samples of plant tissues of the cuttings, which were soaked in the above-described solutions, were taken after 3 days of soaking. The spectra were compared for three variants of samples, that is, hypertrophied lenticels, whose appearance is indicative of active proliferation of cells of plant tissue; dormant lenticels, in which morphological changes were not observed visually (Fig. 1); and phloem (longitudinal section between lenticels). The phloem contains chloroplasts, which generate ROS. Plant-tissue fragments containing lenticels (~2 mm^2 in size, five to six pieces per sample) were excised avoiding the xylem. Figure 1 shows that the adventitious roots grew through the hypertrophied lenticels of the Ledebour willow. This is a well-known situation for woody plants [29–31].

RESULTS AND DISCUSSION

The matrix for planning FFEs in encoded variables and the results of determination of the biometric parameters of rooting of lignified cuttings are shown in Table 1. The mean number and the mean total length of adventitious roots are given. This table also shows data for the control samples, which were soaked in a solution containing IAA but not containing ferrihydrite nanoparticles, as well as in tap water without rooting stimulants (IAA and nanoparticles). In the experiment according to the FFE plan, we used 72 cuttings (three replicates of six cuttings, four rows in the plan). In the experiments corresponding to the central point of the plan we used 108 cuttings.

As can be seen from Table 1, the treatment of the cuttings with biogenic ferrihydrite nanoparticles led to

Table 1. The experiment planning matrix and biometric indices of rooting after the treatment of cuttings with IAA and biogenic ferrihydrite nanoparticles

	Concentration, mg/L	Exposure, h	Number of roots, pcs.	Total length of roots, cm	Number of roots, pcs.	Total length of roots, cm
			on day 5		on day 15	
1	–	–	6	8.8	8	56.7
2	+	–	4	10.0	7	41.3
3	–	+	3	8.0	6	14.7
4	+	+	5	16.2	8	31.7
5	0	0	3.2	5.1	6.2	26.5
Control						
6	IAA		3	4.2	5	23
7	Water		2	2.7	4	18

an increase in the number of adventitious roots on days 5 and 15 of the observations compared to the control samples. This can be seen relative to the mean values for all rows of the table of the results of observations. The difference was at a maximum in the experimental samples (Table 1, rows FFE 1–4) and somewhat lower in the central point of the factorial experiment (Table 1, row 5). Data on the increase in the total length of adventitious roots also show the effect of nanoparticles on the growth of the adventitious roots. Changes in this growth parameter were analyzed using a linear regression equation of the form $Y = b_0 + b_1X_1 + b_2X_2$. In calculating the coefficients of the equation, the total length of the adventitious roots was taken as the Y criterion, because it better corresponds to the surface area of the root system that is responsible for absorbing nutrients and secretion of exudates than the mean root length. For the coded values of variables X_1 and X_2 (± 1), the equation describing the rooting on day 5 took the form

$$Y = 10.8 + 2.3X_1 + 1.4X_2, \quad (1)$$

where Y is the total length of the adventitious roots, X_1 is the concentration of ferrihydrite nanoparticles, and X_2 is the exposure time in the coded units.

Coefficients b_1 and b_2 were calculated on the basis of the results of experiments 1–4 (Table 1) [25]. They quantitatively characterize the effect of factors X_1 and X_2 on the rooting of cuttings (Y) at a significance level of 0.05 and 0.2, respectively. The positive values of the coefficients indicate that an increase in the concentration of nanoparticles and exposure time relative to the central values (1 mg/L and 13 h) should lead to an increase in the total length of the adventitious roots, and vice versa. The b_0 coefficient is the estimated value of the parameter at the central point of FFE, which, calculated according to the results of the experiments, was performed according to the plan (Table 1, rows 1–4). The result of the comparison of the b_0 value with the actual data obtained in the experiments at X_1 and X_2 values of 1 mg/L and 13 h, which correspond to the central point of the plan (Table 1, row 5), characterizes the deviation from linearity.

The mean total length of the adventitious roots on the cuttings that were treated with the solution of ferrihydrite nanoparticles at a concentration of 1 mg/L for 13 h was 5.1 cm. Thus, in the central point of the plan (Table 1, row 5), the observed total length of the roots was two times smaller than the calculated value of 10.8 cm (Eq. (1), coefficient b_0). This means that the dependence of the total root length on the nanoparticle concentration and exposure time is nonlinear and the best conditions for rooting initiation can be reached at a particular combination of the concentration of biogenic ferrihydrite nanoparticles and the exposure time. The rooting efficiency in this case may be much higher than that observed in the experiment. According to Eq. (1), the rooting efficiency of lignified cuttings can be increased by increasing the concentration of nanoparticles (X_1) and the exposure time (X_2) in the initiation solution. However, the search for the optimal conditions for rooting was not performed because the goal of the study was to evaluate the activity of biogenic ferrihydrite nanoparticles. In this regard, it should be noted that the mean total length of the adventitious roots of the control samples (4.2 and 2.7 cm, according to Table 1) is much smaller (2 to 4 times!) than that of the experimental samples that were treated with the nanoparticles (Table 1, rows 1–4).

The biometric parameters of the development of adventitious roots on day 15 are described by the regression equation

$$Y = 36.2 + 0.8X_1 - 12.8X_2. \quad (2)$$

The change in the sign and magnitude of coefficients b_1 and b_2 in Eq. (2) characterizes a prolonged effect of nanoparticles on rooting. The level of signifi-

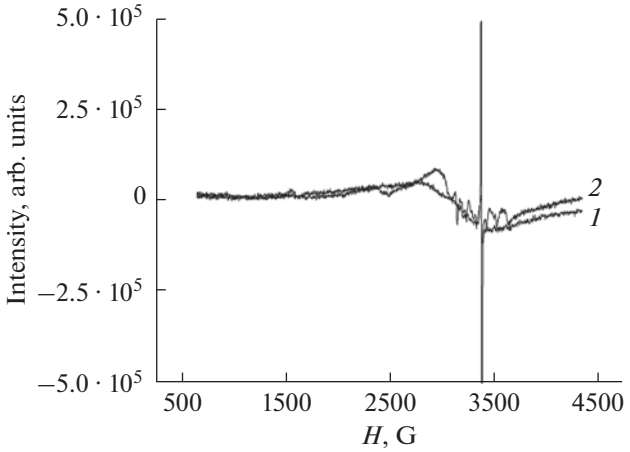

Fig. 2. The EPR spectra of plant tissue of hypertrophied lenticels of cuttings treated with a solution containing IAA: *1*, 295 K; *2*, 90 K.

cance of the coefficient b_2, which gives a quantitative estimate of the effect of the exposure time of cuttings in the nanoparticle-containing solution, increased to 0.05. The significance of the coefficient b_1 decreased; nevertheless, the overall effect of the treatment with nanoparticles remained high. The observations on day 15 showed that the treatment with the biogenic ferrihydrite nanoparticles increased the total length of the adventitious roots by 32% (from 23 to 30.4 cm on average for all rows in the FFE, Table 1) relative to the control experiment with IAA and by 69% relative to the control cuttings that were soaked in water without rooting stimulants.

In the experiment, the mean total length of the adventitious roots in the central point of the FFE plan was 26.5 cm, which is considerably smaller than the calculated value of 36.2 cm (b_0). This means that the nonlinearity of the dependence of the length of adventitious roots on the nanoparticle concentration and exposure time of the cuttings in the solution was less pronounced compared to the dependence observed on day 5, but remained high. The highest value of the total length of the adventitious roots (56 cm), which was observed when the cuttings were incubated in a solution containing nanoparticles at a concentration of 0.5 mg/L for 10 h (Table 1, row 1) was 2.4–3.1 times greater than the control values (23 and 18 cm). Apparently, at the optimal values of factors X_1 and X_2, which can be easily found by experimental design methods [25], the prolonged effect of nanoparticles on the rooting efficiency will also be greater than the mean value that was observed in this experiment (+32%).

Willows easily form roots, especially when rooting is stimulated with growth phytohormones. It is natural to expect that against the background of rooting of the cuttings treated with IAA the effect of any other stimulant (in our case, nanoparticles) will be less pronounced. However, the experimental data obtained for the Ledebour willow showed the biological activity of biogenic ferrihydrite nanoparticles, which is sufficiently high to detect their effect against the background of the growth phytohormone (IAA). The nonlinear dependence of the rooting of cuttings on the concentration of nanoparticle in the soaking solution complicates the determination of the most effective doses of biogenic ferrihydrite nanoparticles and exposure time but does not alter this conclusion. The rooting efficiency of the cuttings treated with the biogenic ferrihydrite nanoparticles was confirmed by the results of their survival when planted in open ground.

It is known that ROS perform signaling functions to initiate the formation and growth of roots as well as other organogenesis processes in plants [20, 32, 33]. Their levels in Ledebour willow tissues were detected using EPR spectroscopy.

The characteristic shape of the EPR spectra of the tissue samples of lignified control and experimental cuttings taken in the initiation period and at the initial stage of growth of the adventitious roots is shown in Figs. 2–4. These figures show the spectra of hypertrophied and dormant lenticels and the phloem, which were recorded 3 days after soaking lignified cuttings in IAA-containing solutions with and without biogenic ferrihydrite nanoparticles.

Figures 2 and 3 show the changes in the EPR spectra that occurred as a result of the treatment of cuttings with nanoparticles added to IAA solution. When the spectra shown in these figures are compared with the spectrum of the phloem (Fig. 4), the changes in the main line (Fe^{3+}) and six lines of the hyperfine structure of Mn^{2+} spectra are clearly seen. The spectra recorded at 295 K have narrow lines at $g \sim 2.0$, which are characteristic of free radicals (ROS). At a temperature of 90 K, the intensity of lines of free radicals is much lower. An opposite picture is observed in the spectra of Mn^{2+}: as the temperature decreases, their intensity increases, especially in EPR spectrum of the phloem (Fig. 4).

The parameters of the lines obtained as a result of modeling the electron magnetic resonance (EMR) spectra, which characterize the state of Fe^{3+} ions in willow tissues, are summarized in Table 2. When modeling the main line of the spectrum, which is ascribed to the Fe^{3+} ion, samples Feh_dl, Feh_hl, Feh_phl, and IAA_dl had two lines at 295 K and three lines (L1, L2, and L3) at 90 K. The experimental spectrum of the IAA_h1 variant is modeled by three lines regardless of the temperature. The spectrum of the IAA_dl sample also contained an L2.1 line with a *g*-factor of 2.5073. Lines L2, L2.1, and L3 indicate that the analyzed plant tissues contained iron atoms in the form of the heme and nonheme iron-containing proteins, whose content and activity changed during the initiation of formation of adventitious roots. In contrast to the L1 line, these lines are characterized by higher val-

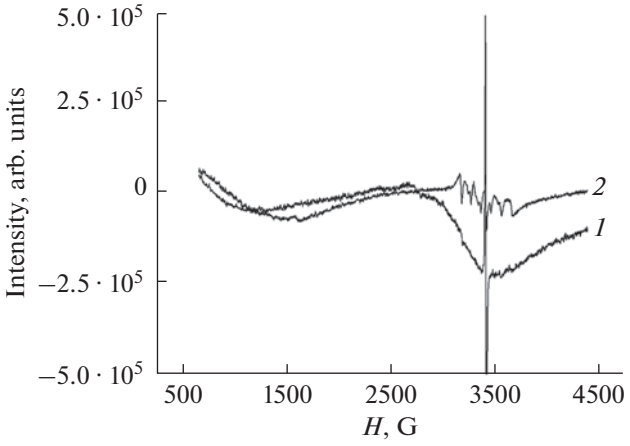

Fig. 3. The EPR spectra of hypertrophied lenticels of cuttings treated with a solution containing IAA and biogenic ferrihydrite nanoparticles: (*1*) 295 K; (*2*) 90 K.

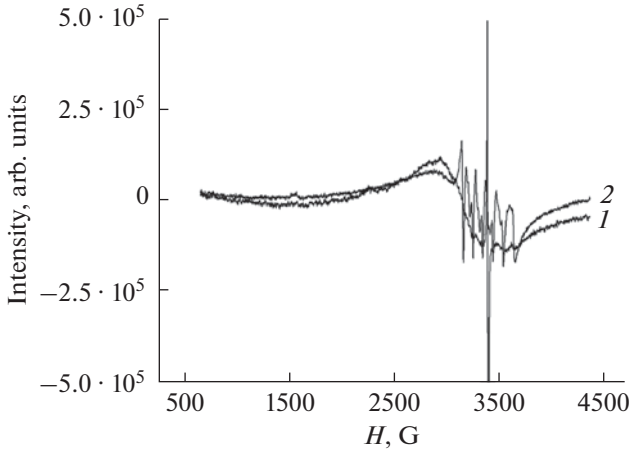

Fig. 4. The EPR spectra of hypertrophied lenticels of cuttings treated with a solution containing biogenic ferrihydrite nanoparticles: (*1*) 295 K; (*2*) 90 K.

ues of the *g*-factor. They also differ in other parameters, namely, in the width (*DH*) and intensity (*I*) of the lines (Table 2). Without dwelling on the identification of various biological compounds that contain iron ions, we consider the changes in the parameters of the spectra that show the effect of biogenic ferrihydrite nanoparticles on the rooting of lignified cuttings of Ledebour willow.

In the EMR spectra of lenticels and phloem, which were taken from the cuttings treated with the nanoparticles, the value of the *g*-factors of the L1 lines at 295 K was 2.1112–2.139. At 90 K, the values of the *g*-factors decreased to 2.0423–2.099. The intensity of the L1 lines also decreased (Table 2). This pattern was not observed in the EMR spectra of IAA-h1 and IAA_dl lenticels, which were taken from the cuttings that were not treated with nanoparticles. The observed temperature dependence of *g*-factors of the L1 lines indicates that the Fe^{3+} ion was in the superparamagnetic state. This fact indicates that biogenic ferrihydrite nanoparticles containing iron ions in the superparamagnetic state were transported to all analyzed plant tissue samples of willow cuttings that were soaked in the nanoparticle-containing solution.

The plant tissues of the willow cuttings that were not treated with nanoparticles may contain ferritin, which contains endogenous ferrihydrite with Fe^{3+} ions in the superparamagnetic state. However, the intensity of the L1 line in Feh_hl and Feh_dl samples was significantly higher than that in IAA_h1 and IAA_dl samples (Table 2) because the former contained synthetic nanoparticles, which were introduced when the cuttings were soaked in the initiation solution, and a relatively low concentration of endogenous ferrihydrite.

The intensity of the L2 lines at 295 K is much smaller, while the *g*-factor value is higher (2.223–2.923). At 90 K, the intensity of the L2 lines was also smaller and the *g*-factor was determined in the 2.326–2.602 range (Table 2). We did not record lines with a *g*-factor of 2.3–2.9 in the EMR spectra of biogenic ferrihydrite nanoparticles [27]. These characterize the iron ions in the octahedral environment, which are likely to be the components of prosthetic groups of various proteins. At 90 K, signals with a lower intensity with *g*-factor values of 4.28–4.45 were also observed (Table 2, L3 lines), which are characteristic of the Fe^{3+} ions in the tetrahedral or strongly distorted octahedral environment and are components of nonheme iron–sulfur proteins. We did not observe iron atoms in the tetrahedral environment in the EMR spectra of the biogenic ferrihydrite nanoparticles [27].

The EMR spectrum of the phloem recorded at the low temperature differed from the spectra of the lenticels that were treated with nanoparticles in that, regardless of the temperature, the experimental spectrum was modeled by only two lines. At 295 K, the EMR spectra of the lenticels that were taken from the cuttings treated with nanoparticles were also modeled by two lines. However, the values of the parameters (*g*-factor, width, and intensity) of the lines differed significantly. Apparently, this was due to the differences in the content and activity of metal-containing proteins in the cells of the phloem and lenticels, as well as to the initiation and growth of the adventitious roots. The iron atoms, which are characterized by the L2 and L3 lines, are associated with biological structures and are not components of the mineral part of the samples (i.e., biogenic ferrihydrite nanocrystallites).

The primary effects of biogenic ferrihydrite nanoparticles on the formation of adventitious roots manifest themselves most strongly in the intensity of lines of free radicals and manganese ion (Mn^{2+}) in the EPR spectra. The results of the comparative analysis

Table 2. The results of decomposition and determination of parameters of calculated lines of EMR spectra of plant tissues of lignified cuttings of the Ledebour willow

Line no.	Sample type					Parameter
	Feh_phl	Feh_hl	Feh_dl	IAA_hl	IAA_dl	
L1	2.139	2.1112	ND	2.1125	2.0198	*g*-factor, 295 K
L2	2.923	2.415		2.223	2.223	
L2.1				2.8		
L1	2.099	2.0423	2.0433	2.152	2.1066	
L2		2.602	2.381	2.326	2.3258	*g*-factor,
L2.1					2.5073	90 K
L3	4.28	4.45	4.251	4.285	4.28	
L1	484.5	405.7	ND	516.5	311.8	
L2	77.2	534.2		131	417.8	*DH*, E
L3				194		295 K
L1	561.5	618	466.7	524.9	512.7	
L2		688	308.4	612	220.7	*DH* , E
L2.1					564	90 K
L3	32.4	46	96	45.2	53.6	
L1	243687	187427	ND	130298	155799	
L2	11733	119088		58602	209496	*I*, arb. units
L3				25432		295 K
L1	153229	102478	106150	63132	68113	
L2		53292	50505	35972	28691	*I*, arb. units
L2.1					39665	90 K
L3	23495	13118	8351	17201	12802	

NR, spectrum was not recorded; IAA, cuttings treated with IAA solution; Feh, cuttings treated with IAA solution and biogenic ferrihydrite nanoparticles (indices phk, dl, and hl designate variants of samples, phloem, dormant and hypertrophied lenticles, respectively).

of the intensities of lines of free radicals and manganese are summarized in Table 3. The ranking of the lines of free radicals correlates with the initiation of growth processes (Feh_dl > Feh_hl > IAA_h1 > IAA_ dl ⩾ Feh_phl) (Table 3). When rooting was initiated using IAA only, the intensity of lines of free radicals in the EPR spectrum was lower than that in the samples of the cuttings that were additionally treated with ferrihydrite nanoparticles. The higher intensity of the line of free radicals in the dormant lenticels (Feh_dl) was probably due to the fact they were at the initial stage of the initiation of proliferation of the meristematic cells of the adventitious roots, which was not observed externally (Fig. 1) but the level of the signal that triggers their formation is at a maximum. It should be noted that the initial period of the early response of plant cells (cuttings) to the treatment with nanoparticles was detected using the EPR analysis. In the phloem samples, free radicals practically were not observed. This was possibly due to the fact that, in contrast to the cells of lenticels and accompanying meristematic cells, which were at the stage of rooting initiation, the phloem cells did not actively proliferate in the observation period. Earlier, we showed that the biogenic ferrihydrite nanoparticles exhibited biological activity regardless of the presence of IAA. In particular, they increased the germination capacity and growth of roots of oat seeds [34] and the generation of ROS in rat liver cells [35].

The intensity of manganese lines in the samples of the phloem (Feh_phl) and dormant lenticels (Feh_dl) that were treated with the nanoparticles was 3–4 times higher than that in the samples of hypertrophied lenticels (Feh_hl) and those treated with IAA only (Table 3). The first line in the low-field part of the EPR spectrum of manganese was selected as a marker of the intensity of the hyperfine-structure lines. The higher intensity of manganese lines in the spectrum of the dormant lenticels (Feh_dl) compared to that of the hypertrophied lenticels (Feh_hl) treated with the nanoparticles can be explained in the same manner as that of the signal intensity of free radicals. It can be concluded that the intensity of the hyperfine-structure lines in the EPR spectrum of manganese also correlated with the initiation of growth processes: Feh_dl ⩾ IAA_h1 ≈ Feh_hl ≈ IAA_dl (Table 3).

Table 3. Intensities of lines of the hyperfine structure of Mn^{2+} and radical center in the EPR spectra of plant tissues of lignified cuttings of Ledebour willow (at 90 K)

Sample	Mn^{2+} line intensity, arb. units	Free radical line intensity, arb. units	Intensity rank of free radical line	Intensity rank of Mn^{2+} line
Feh_fl	333572	~0	–	1
Feh_dl	278902	301181	1	2
Feh_hl	81651	154355	2	4
IAA_hl	89211	130070	3	3
IAA_dl	81224	103621	4	5

We assumed that the manganese ions in the lenticel samples are present in the active site of the manganese-containing superoxide dismutase (Mn-SOD). The manganese ion in the active center of Mn-SOD cyclically changes its valence ($Mn^{2+} \leftrightarrow Mn^{3+}$) in the two-stage reaction of disproportionation of the superoxide radicals [36]. At the low temperature (90 K), the steady-state of Mn-SOD may be shifted towards the reduced state of the enzyme (Mn^{2+} ion), whereas at 295 K it is shifted towards the oxidized state (Mn^{3+} ion). Since the spectrum of Mn^{3+} is almost not recorded under our conditions, the intensity of manganese lines at 295 K is lower. Apparently, the antioxidant system in the analyzed cells of lenticels is most strained; hence, the activity of Mn-SOD is high. A similar pattern of changing the intensity of the EPR signal from Mn^{2+} ions depending on temperature was observed in [37]. However, the authors of [37] did not associate this fact with the presence of Mn-SOD in germinating wheat grains. The maximum intensity of manganese lines was detected in the phloem sample. This was due to the fact that the phloem contains chloroplasts and manganese ions are present in the active site of the photosystem II complex, which is involved in the photolysis of water [38]. It is therefore highly likely that they contribute to the intensity of the EPR signal characteristic of the Mn^{2+} ion.

In general, the comparison of the results of the biometric analysis of rooting of lignified cuttings of Ledebour willow with the results of analysis of plant tissues at the initial stage of rooting that were obtained by electron paramagnetic resonance clearly shows that the biogenic ferrihydrite nanoparticles have a stimulatory effect on the formation of adventitious roots. The initiation of growth of root-forming meristematic cells should be accompanied by an elevated level of ROS [32, 33, etc.]. In accordance with this concept, the analysis of EPR spectra showed that in the period of rooting activation when the lignified cuttings were soaked in the IAA solution containing biogenic ferrihydrite nanoparticles the cells of the plant tissue (lenticels) are characterized by an increased level of free radicals (ROS) and the signal of the EPR spectrum of Mn^{2+} ion.

ACKNOWLEDGMENTS

This study was supported by the Russian Foundation for Basic Research, the Government of the Krasnoyarsk krai, and the Krasnoyarsk regional foundation for support of scientific and technical activities under the research project no. 16-48-242158.

REFERENCES

1. C. Remédious, F. Rosário, and V. Bastos, J. Bot., Article ID 751686 (2012).
2. B. Ruttkay-Nedecky, O. Krystofova, L. Nejdl, and V. Adam, J. Nanobiotechnol. **15** (33), (2017).
3. A. M. Korotkova, S. V. Lebedev, F. G. Kayumov, and E. A. Sizova, S-kh. Biol. **52** (1), 182 (2017).
4. V. M. Yurin and O. V. Molchan, Tr. Belarus. Gos. Univ. **10** (1), 9 (2015).
5. P. P. Fu, Q. S. Xia, H. M. Hwang, et al., J. Food Drug. Anal. **22**, 64 (2014).
6. Yu. N. Vodyanitskii, *Iron Compounds and Their Role in Soil Conservation* Nauka, Moscow, 2010) [in Russian].
7. R. M. Cornell and U. Schwertmann, *The Iron Oxides* (Wiley, Weinheim, 2003).
8. K. Eusterhues, T. Rennert, H. Knicker, et al., Environ. Sci. Technol. **45** (2), 527 (2011).
9. A. Violante and A. G. Caporale, J. Soil Sci. Plant Nutr. **15** (2), 422 (2015).
10. C. W. Childs and Z. Pflanz. Bodenkunde **155** (5), 441 (1992).
11. C. M. Jonsson, P. Persson, S. Sjöberg, and J. S. Loring, Environ. Sci. Technol. **42** (7), 2464 (2008).
12. E. Čadková, M. Komárek, R. Kaliszová, et al., Environ. Sci. Pollut. Res. Int. **20** (6), 4205 (2013).
13. T. Xia, M. Kovochich, J. Brant, et al., Nano Lett. **6** (8), 1794 (2006).
14. K. Jeyasubramanian, U. U. G. Thoppey, G. S. Hikku, et al., RSC Adv. **6**, 15451 (2016).
15. D. V. Kolbanov, E. O. Legerova, I. I. Donskaya, et al., in *Biotechnological Approaches to Palnt Biodiversity Conservation and Selection: Proc. Int. Conf.* (Monsk, 2014), pp. 114–117 [in Russian].
16. J. Dat, S. Vandenabeele, E. Vranová, et al., Cell. Mol. Life Sci. **57**, 779 (2000).
17. T. P. Astafurova, Yu. N. Morgalev, A. P. Zotikova, et al., Vestn. Tomsk. Gos. Univ., Ser. Biol. **1** (13), 122 (2011).

18. X. J. Xia, Y. H. Zhou, K. Shi, et al., J. Exp. Bot. **66** (10), 2839 (2015).
19. B. Wang, J.-J. Yin, X. Zhou, et al., J. Phys. Chem. C **117** (1), 383 (2013).
20. V. D. Kreslavski, D. A. Los, S. I. Allakhverdiev, and Vl. V. Kuznetsov, Russ. J. Plant Physiol. **59** (2) 141, (2012).
21. Yu. A. Labas, A. V. Gordeeva, Yu. I. Deryabina, et al., Usp. Sovrem. Biol. **130** (4), 323 (2010).
22. S. Choudhury, P. Panda, L. Sahoo, and S. K. Panda, Plant Signal Behav. **8** (4), 751686 (2013).
23. S. Mangano, S. P. D. Juárez, and J. M. Estevez, Plant Physiol. **171**, 1593 (2016).
24. M. T. Tarasenko, *Plant Propagation by Green Grafts* (Kolos, Moscow, 1967) [in Russian].
25. V. N. Maksimov, *Multifactor Experiment in Biology* (Moscow State Univ., Moscow,1980) [in Russian].
26. V. F. Moiseychenko, *Methodology of Experimentation in Pomiculture and Horticulture* (Vishcha Shkola, Kiev, 1988) [in Russian].
27. M. I. Teremova, E. A. Petrakovskaya, A. S. Romanchenko, et al., Environ. Progr. Sustain. Energy **35** (5), 1407 (2016).
28. Yu. L. Gurevich, S. V. Markov, Yu. I. Man'kov, et al., in *Ultrafine Powders, Nanostructures, and Materials: Proceedings of Scientific-Technical Conf. with International Participation* (Krasnoyarsk, 2015), pp. 98–101 [in Russian].
29. A. R. S. Gomes and T. T. Kozlowski, Plant Physiol. **66**, 267 (1980).
30. K. Haase, O. D. E. Simone, J. J. Wolfgang, and S. Wolfgang, Tree Physiol. **23**, 1069 (2003).
31. Y. A. Kuzovkina, M. Knee, and M. F. Quigley, J. Environ. Hort. **22** (3), 155 (2004).
32. M. J. Bennett, C. Perilleux, T. Beeckman, and X. Draye, Development **143**, 3328 (2016).
33. G. Gapper and L. Dolan, Plant Physiol. **141**, 341 (2006).
34. D. I. Shevelev, S. V. Khizhnyak, Yu. L. Gurevich, and M. I. Teremova, Usp. Sovrem. Nauk **5** (2), 57 (2017).
35. V. G. Pakhomova, K. V. Shadrin, G. V. Makarskaya, et al., Zdorov'e Med. Ekol. Nauka **70** (3), 136 (2017).
36. A.-F. Miller, FEBS Lett. **586** (5), 585 (2012).
37. M. Filek, M. Łabanowska, M. Kurdziel, and A. Sieprawska, Toxins **9** (6), 178 (2017).
38. M. M. Najafpour, M. Z. Ghobadi, B. Haghighi, et al., Biochemistry (Moscow) **79** (4), 324 (2014).

Translated by M. Batrukova